Bond behavior of GFRP bars in concrete with carbon nanotubes

Elvys Dias Reis, Péter Ludvig, Fabrice Gatuingt, Flávia Spitale Jacques Poggiali, Augusto Cesar da Silva Bezerra

CICE 2023 Rio de Janeiro – Brazil 11TH INTERNATIONAL CONFERENCE ON FRP COMPOSITES IN CIVIL ENGINEERING

BOND BEHAVIOR OF GFRP BARS IN CONCRETE WITH CARBON NANOTUBES

Elvys D. Reis, Federal Center for Technological Education of Minas Gerais, Brazil,
elvysreis@yahoo.com.br
Péter Ludvig, Federal Center for Technological Education of Minas Gerais, Brazil,
peter@cefetmg.br
Fabrice Gatuingt, Université Paris-Saclay, France,
fabrice.gatuingt@ens-paris-saclay.fr
Flávia S. J. Poggiali, Federal Center for Technological Education of Minas Gerais, Brazil,
flaviaspitale@gmail.com
Augusto C. S. Bezerra, Federal Center for Technological Education of Minas Gerais,
augustobezerra@cefetmg.br

ABSTRACT
This work investigates the adherence of 12.7 mm glass fiber-reinforced polymer (GFRP) bars in concrete with carbon nanotubes (CNT) through pull-out tests. Eighteen specimens were used to investigate the impact of CNT content (0% and 0.05% by weight of cement) and anchorage length (5d and 10d). Reference samples were produced using 12.5 mm steel bars. An additional fifty-four specimens were cast to evaluate the influence of CNTs on the mechanical and durability properties of the concrete. This research provides satisfactory results regarding utilizing GFRP bars instead of steel ones and incorporating CNT in concrete.

Graphical abstract

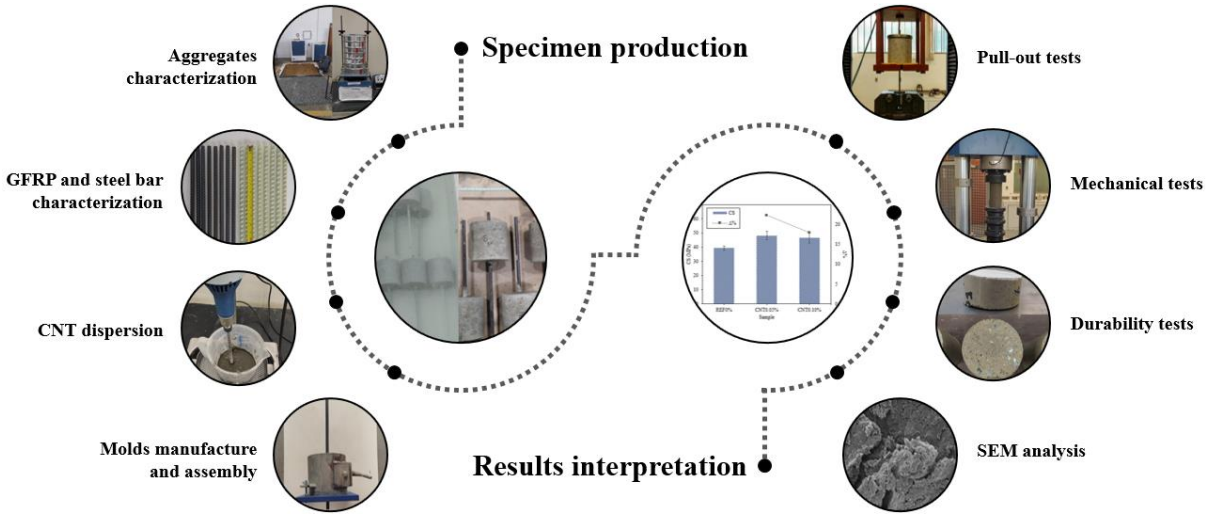

KEYWORDS
Bond strength. Cement-based materials. Nanotechnology. Sustainability.

INTRODUCTION
Concrete is one of the most widely used materials in civil construction, and nanotechnology offers several possibilities for improving its properties, one of them being the use of nanoparticles to enhance the strength and durability of the material (Van Tonder & Mafokoane, 2014). Due to their minimal size, nanoparticles can fill the voids between the larger cement, aggregate, and sand particles, resulting in a more compact and resistant concrete structure. The small particles serve as nucleation sites for cement

hydration products, which may lead to similar enhancement of the cement matrix. In addition, nanoparticles can prevent the penetration of aggressive agents, such as water and chemicals, that can cause long-term damage to concrete (Ahmed et al., 2019). Using more durable concrete can help reduce waste generation, promoting sustainability by reducing the environmental and economic impacts of waste generation and disposal in the construction industry (Vieira et al., 2019).

Carbon nanotubes (CNTs) are promising for improving concrete strength and durability. CNTs are tubular carbon structures with diameters in the order of nanometers, with exceptional mechanical properties, such as high strength and stiffness (Liew et al., 2016). For this reason, several researchers have directed efforts to investigate their application in concrete (Han et al., 2023). However, incorporating these structures in concrete is still a technological challenge, which requires developing techniques for the dispersion and alignment of these materials in concrete (Jung et al., 2020; Reis et al., 2022).

In the case of reinforced concrete, steel bars are the most commonly used material as reinforcement due to their mechanical properties and ease of forming. However, using steel bars in reinforced concrete presents disadvantages, such as its susceptibility to corrosion, high density, and waste generation (Yu et al., 2020). Thus, it is essential to adopt preventive measures to minimize these problems, such as applying protective coatings on steel bars (Wu et al., 2019), using construction techniques that reduce waste generation (Martins et al., 2022), and using alternative materials for concrete reinforcement, such as glass-fiber reinforced polymers (GFRP) (Raza & Rafique, 2021).

GFRP bars are an alternative to steel for concrete reinforcement, presenting several advantages over traditional materials, such as corrosion resistance, lightness, high strength, and durability (Benmokrane et al., 2021). It is also essential to emphasize the sustainable aspect of GFRP bars since they are made of recyclable materials, just like steel (De Fazio et al., 2023), the latter having a large-scale recycling process already consolidated, which is not yet the case with polymers. However, it is still a relatively new alternative in the market and may require adaptations in construction techniques and applicable technical standards.

With this perspective, the study of bonding between bars and concrete is significant to ensure the effectiveness of the strengthening system. The adherence refers to the ability of the bars to bond to the concrete and transfer the forces applied between the materials (Xiong et al., 2021). In the case of GFRP bars, the adherence between them and the concrete is essential to ensure uniform and efficient distribution of the load applied to the structure and its resistance to external and internal forces (Liu et al., 2023). The adhesion between FRP bars and concrete depends on many factors, such as the bar diameter, anchorage length, and concrete type. The additions to the cementitious matrix aim to improve its properties and positively influence its adhesion to the reinforcement bars. The topic still requires further research, even though it is being increasingly investigated (Reis et al., 2023).

Considering the potential of using nanotechnology and alternative materials in civil construction to develop more resistant, durable, and sustainable structures, besides contributing to reducing the environmental impact caused by the construction industry, this paper aims to investigate the bond behavior of GFRP bars in concrete with carbon nanotubes (CNT-concrete), as well as the mechanical and durability properties of CNT-concrete. Specifically, this manuscript answers the following questions: What are the effects of CNT incorporation on the (i) compressive and tensile strength, (ii) static and dynamic modulus of elasticity, and (iii) porosity and water absorption of concrete? (iv) What does adding CNT to concrete influence its bond strength with GFRP bars? To this end, an experimental campaign and future research directions were presented.

MATERIALS AND METHODS

Materials

The materials used in the concrete production were: (i) Brazilian Type CPV-ARI RS Portland cement—cement with low content of additions in its chemical composition and a high degree of fineness—

produced by Holcim, with physical and mechanical properties shown in Table 1; (ii) natural sand (fine aggregate, FA) with a fineness modulus of 2.75 and a maximum diameter of 2.4 mm, characterized according to NBR NM 248 (ABNT, 2003), and a specific gravity of 2.632 g/cm^3, characterized according to NBR 9776 (ABNT, 1987); (iii) gneiss gravel (coarse aggregate, CA) with a fineness modulus of 4.92 and a maximum diameter of 9.5 mm (ABNT, 2003), and a specific gravity of 2.646 g/cm^3 (ABNT, 1987); (iv) MWCNTs (only for CNT–concrete samples) selected from the CTNano, Brazil. They were synthesized by chemical vapor deposition (CVD) and present estimated lengths between 5 μm and 30 μm, external diameter between 10 and 30 nm, and purity greater than 93%—complete specifications described in the nanomaterial data sheet (NanoView, 2022). The isopropanol used to disperse the CNTs was the absolute grade of the EMFAL brand; (v) FRP bars of 12 mm diameter, a tensile strength of 917 MPa, 0.8d–1.2d rib spacing (e), and rib inclination (β) ≥ 60°, as indicated in Figure 1—detailed specifications in the manufacturer data sheet (Stratus, 2019); (vi) ribbed steel bars of 12.5 mm diameter (d), a yield point of 591 MPa, a tensile strength of 674 MPa, 0.02d–0.04d rib height, 0.5d–0.8d rib spacing (e), and rib inclination (β) ≥ 45°, as shown in Figure 1; (vii) superplasticizer (SP) and hydration stabilizer (HS) additives in water suspension, whose specifications are in Table 2. The choice of a polycarboxylate-type SP is worth mentioning because the cement and calcium ions' alkaline medium directly influences nanomaterials' agglomeration. Chuah et al. (2018), for example, used a polycarboxylate-type SP to disperse graphene oxide and obtained promising results.

Table 1. Physical and mechanical properties of CPV-ARI RS Portland cement

Test type		Characteristic		Reference standard	Limit
Specific area—Blaine (cm^2/g)		4620		NBR 16372 (2015)	≥ 3000
Setting time (mins)	Start	135		NBR 16607 (2018)	≥ 60
	End	205		NBR 16607 (2018)	≤ 600
Compressive strength (MPa)		1 day	19.6	NBR 7215 (2019)	≥ 14.0
		3 days	31.8	NBR 7215 (2019)	≥ 24.0
		7 days	41.3	NBR 7215 (2019)	≥ 34.0
		28 days	52.4	NBR 7215 (2019)	–

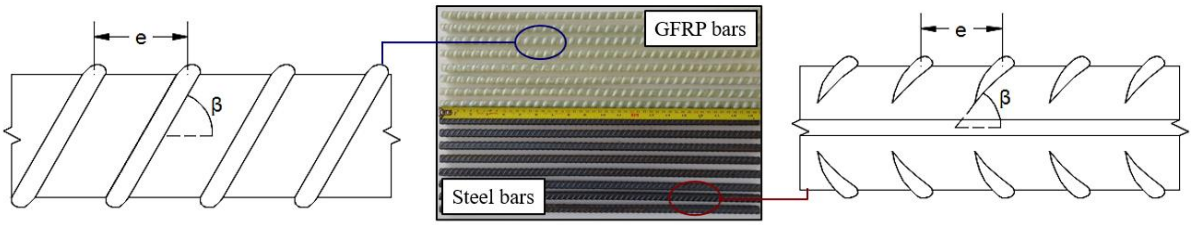

Figure 1: Geometric characteristics: (a) GFRP bar; (b) steel bar

Table 2. Properties of superplasticizer and hydration stabilizer additives

Property	Superplasticizer	Hydration stabilizer
Name	Sika® ViscoCrete®–5800 FTN	Matchen stabilizer
Aspect at 25 ºC	Brown liquid	Blue liquid
pH	4.5 ± 1.0	3.5–5.5
Density at 25 ºC (g/cm^3)	1.07 ± 0.02	1.035–1.095
Suggested content	0.2%–2.0%	–

CNT dispersion

The dispersion method was the pre-dispersion of CNTs on cement particles in an isopropanol medium, a proven effective process in previous research (Makar & Chan, 2009; Rocha & Ludvig, 2018). The method consisted of three steps: (i) CNTs and approximately 200 ml of isopropanol were added to a glass container, shaken at 10.000 rpm, and sonicated on ultrasonic apparatus with 42 kHz frequency for 30 minutes; (ii) ten percent of the cement mass and another 200 ml of isopropanol were incorporated into the mixture, which was transferred to a plastic container and mechanically stirred and sonicated for

additional 90 minutes; (iii) in a glass container, drying in an oven at 100±5 ºC for 24 hours, leaving only a visually homogeneous dry power of cement particles coated with CNTs. The resulting dry mixture was then mixed with the remaining cement to prepare the CNT–concrete samples before adding water. Figure 2 details the dispersion process.

(a) (b) (c) (d) (e) (f)

Figure 2: CNT dispersion steps: (a) weighing of CNTs and cement; (b) CNTs ultrasonication in isopropanol; (c) mechanical stirring of CNTs and cement in isopropanol; (d) oven drying of the mixture; (e) aspect of the dry mixture; (f) mixing of the dispersed CNTs with the remaining cement

Mixture compositions and specimen production

The concrete samples were prepared in the Laboratory of Construction Materials, Structures, and Components of the Federal Center for Technological Education of Minas Gerais (CEFET–MG). The concrete mixes in Table 3 were produced with a w/c ratio of 0.53 for a target slump class S160 and compressive strength Group I (30 MPa) according to NBR 8953 (ABNT, 2015). For the CNT–concrete samples, the contents of MWCNTs were limited to 0.05% ($CNT_{0.05}$) and 0.10% ($CNT_{0.10}$) by weight of cement to avoid agglomeration (Hassan et al., 2019). Concrete without CNTs (REF) was also produced as a reference for comparison purposes.

Table 3: Concrete mix design

Sample	Cement (kg/m^3)	Aggregates (kg/m^3)		Water (kg/m^3)	Additives (kg/m^3)		CNT (%wc)
		FA	CA		SP	HS	
REF	384	960	838	204	0.80	0.26	0.00
$CNT_{0.05}$	384	960	838	204	0.80	0.26	0.05
$CNT_{0.10}$	384	960	838	204	0.96	0.26	0.10

The mixture was produced using a 120 L concrete mixer in three steps: (i) a small amount of water was added to moisten the inside surface of the mixer; (ii) the aggregates were mixed with 60% of the total mixing water for three minutes; (iii) the cement (with or without CNTs), SP and HS additives, and the remaining 40% of mixing water were added and mixed for additional five minutes. The slump test followed the recommendations of NBR NM 67 (ABNT, 1998) to measure concrete consistency. Eighteen cylindrical pull-out specimens measuring 150 mm diameter and 150 mm in length were prepared. FRP and steel bars were embedded in the center of the concrete specimens—according to the literature, the cover-to-bar diameter greater than five (C/d > 5) is more likely to lead to pullout failure (Carvalho et al., 2018), as desired in this research. Bond lengths of five and ten times the bar diameter (5d and 10d) were adopted. The bar verticality was ensured using a styrofoam plate with 30 mm thick holes under the cylindrical molds' 20 mm thick wooden base. Figure 3 presents the pull-out test setup and the molded specimen, and Table 4 summarizes the corresponding test program. Fifty-four specimens 100 mm in diameter and 200 mm long were produced for the mechanical and durability tests, eighteen of each mixture. The properties studied were compressive strength, static modulus of elasticity, dynamic modulus of elasticity, tensile strength, porosity, and water absorption. All specimens were cast at the same time, de-molded after 24 h, and cured in saturated calcium hydroxide solution at 23 ± 2 °C for 28 days, as recommended by NBR 5738 (ABNT, 2015b).

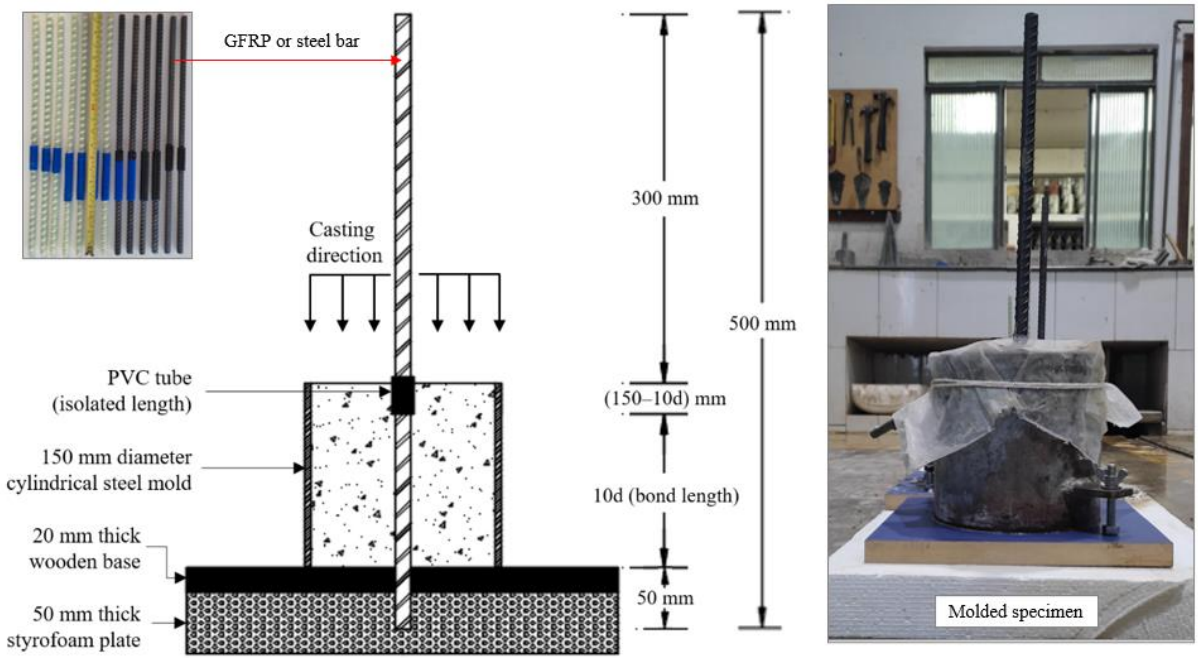

Figure 3: Pull-out test setup and the molded specimen (10d bond length case)

Table 4: Details of pull-out test program

Specimen designation	Bar type	CNTs (%wc)	Diameter (mm)	Bond length (mm)	Specimens
G-0.05-12-5d	GFRP	0.05	12.0	60.0 (5d)	3
G-0.00-12-5d	GFRP	0.00	12.0	60.0 (5d)	3
G-0.00-12-10d	GFRP	0.00	12.0	120 (10d)	3
S-0.05-12.5-5d	Steel	0.05	12.5	62.5 (5d)	3
S-0.00-12.5-5d	Steel	0.00	12.5	62.5 (5d)	3
S-0.00-12.5-10d	Steel	0.00	12.5	125 (10d)	3

Test procedures

Figure 4 provides an overview of the tests, indicating the reference procedure, the related equipment, and the number of specimens. Care was taken to ensure that the conditions for all tests were the same, and the specimens were chosen randomly to represent the samples best.

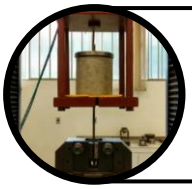

Bond strength
Method: Pull-out test—RILEM-RC-6 (RILEM, 1983; Carvalho et al., 2018)
Equipment: Universal Testing Machine—EMIC PC 200 CS Model
Specimens: 18 (3 per sample)

Compressive strength
Method: Compression test—NBR 5739 (ABNT, 2018)
Equipment: Universal Testing Machine—EMIC PC 200 CS Model
Specimens: 9 (3 per sample)

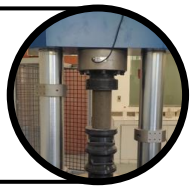

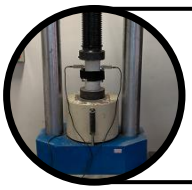

Static modulus of elasticity
Method: Static compression test
Equipment: Universal Testing Machine—EMIC PC 200 CS Model
Specimens: 9 (3 per sample)

Dynamic modulus of elasticity
Method: Natural resonance frequency—ASTM E1876 (ASTM, 1983)
Equipment: Erudite MKII equipment
Specimens: 18 (6 per sample)

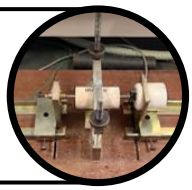

Splitting tensile strength
Method: Diametral compression (Lobo Carneiro test)—NBR 7222 (ABNT, 2011)
Equipment: Universal Testing Machine—EMIC DL 30000 Model
Specimens: 9 (3 per sample)

Porosity
Method: Surface pore area of scanned cross-sections (Mendes et al., 2017)
Equipment: Scanner and MATLAB code developed by Rabbani et al. (2014)
Specimens: 24 (8 per sample)

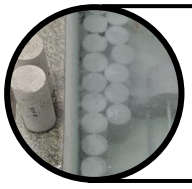

Water absorption
Method: Saturated and dry mass ratio—NBR 9778-2 (ABNT, 2009)
Equipment: Model CE 220/150 oven and Model LD 2051 balance
Specimens: 27 (9 per sample)

Figure 4: Overview of the tests and details of the procedures

Statistical analysis

Tukey's means contrast test, with a significance level of 5%, was used to examine the impact of the individual factor (CNT content). In Tukey's test, A represents the sample with the highest mean value for a specific property, B corresponds to the second highest mean value, and so on. Treatments with the same letter indicate statistically equivalent means. The Anderson-Darling normality test (at a 5% significance level) was used to validate the Tukey test results, with a p-value greater than or equal to the significance level, implying a normal distribution condition.

RESULTS AND DISCUSSIONS

Mechanical and durability properties

Figure 5 presents the mean values, extreme coefficients of variation (CV), mean confidence intervals (CI – 95% reliability), and the results of Tukey's means contrast test (5% significance) for the evaluated properties. The p-values of the Anderson-Darling (AD) normality test ranged from 0.092 to 0.673, validating the Tukey test results (p-value ≥ 0.05).

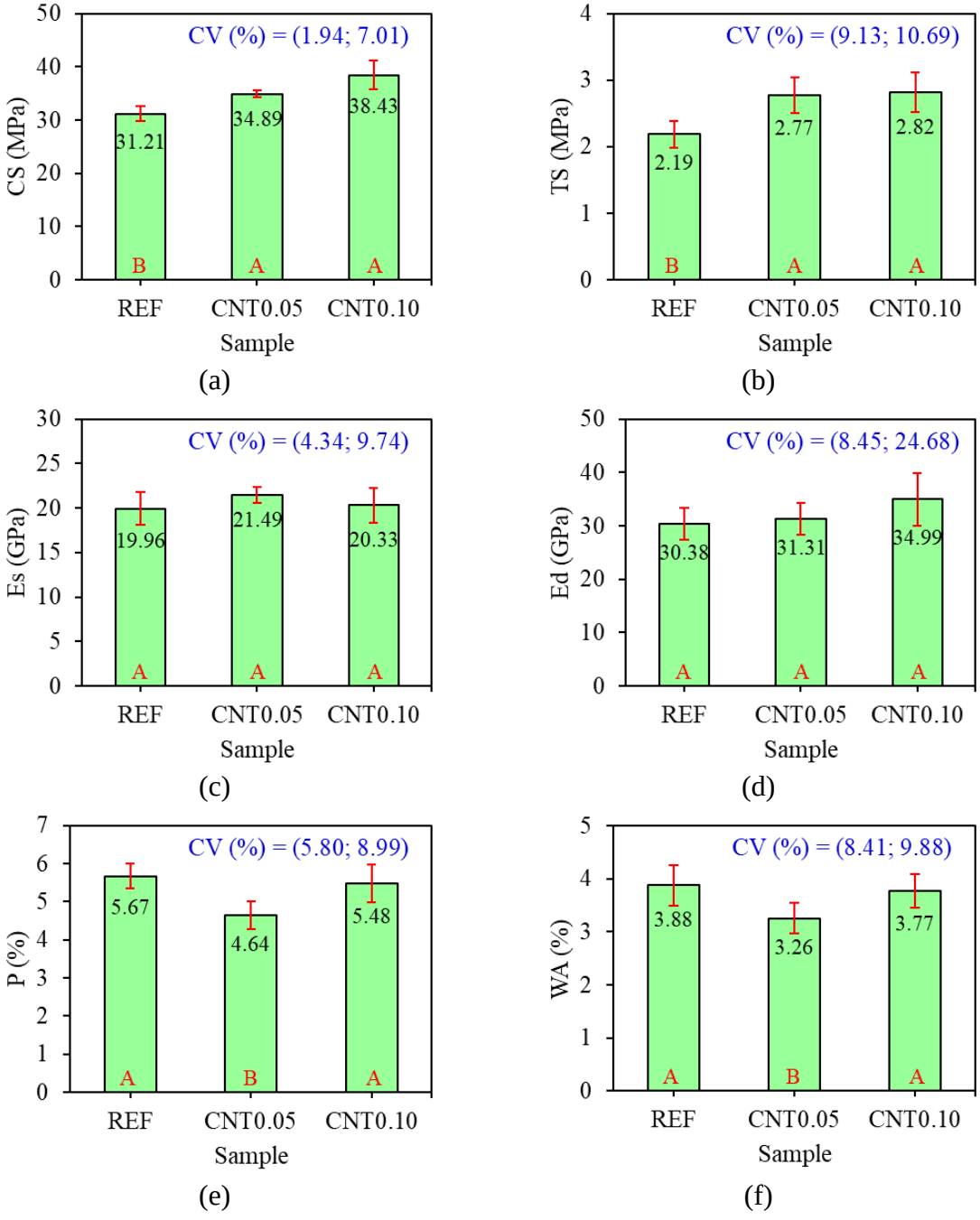

Figure 5: Test results for mechanical and durability properties: (a) CS—Compressive strength; (b) TS—Tensile strength; (c) Es—Static modulus of elasticity; (d) Ed—Dynamic modulus of elasticity; (e) P—Porosity; (f) WA—Water absorption

The results of Tukey's test indicated statistically significant improvements in the CS relative to the reference sample when 0.05% CNT (12% increase) and 0.10% CNT (23% increase) were added to the

mix (Figure 5a). The same pattern occurred with TS, with increases of 26% (CNT0.05) and 29% (CNT0.10) relative to CNT-concrete (Figure 5b). In the case of Es (Figure 5c) and Ed (Figure 5d), adding CNTs to the cement matrix did not lead to significant effects, with the Tukey test indicating equivalent means for the three samples. The results of P (Figure 5e) and WA (Figure 5f), on the other hand, showed a positive effect of the addition of 0.05% CNT to concrete, with reductions of 18% and 16%, respectively, concerning plain concrete. According to Tukey's test, the content of 0.10% CNT resulted in P and WA equivalent to the reference sample.

The increase in CS and TS caused by CNTs can generally be explained by the nucleation effect, which facilitates the cement hydration reaction. In addition, CNTs can act as bridges for stress transfer between cracks and voids, contributing to this increase (Konsta-Gdoutos et al., 2019). However, it is essential to mention that a high proportion of CNTs can lead to agglomeration and coating of the material surface, hindering the hydration reaction. The compressive and tensile strengths may decrease below the maximum values in this case (Jung et al., 2020). In addition, CNTs positively affect the pore structure of concrete because they can fill capillary pores and the voids between cement hydration products, which results in advantages in terms of concrete durability, such as the reduction of P and WA (Xu et al., 2015).

Therefore, adding 0.05% CNT to concrete positively affected CS, TS, P, and WA. However, there was no significant impact on Es and Ed. As reported by the literature, CNTs are more difficult to disperse in high concentrations. They may agglomerate due to van der Walls forces and generate large pores in the cementitious composite, which worsens its mechanical properties (Gillani et al., 2017). With this in mind and knowing that CNTs are not yet industrially scaled and therefore are expensive, this research indicates that future research should avoid using contents higher than 0.05% CNT.

Bond slip behavior

Maximum bond strength

Figure 6 displays the mean values, extreme CV, mean CI (95% reliability), and the results of Tukey's means contrast test (5% significance) for the maximum bond strength (τ_b). The p-values of the AD normality test ranged from 0.119 to 0.293, validating the Tukey test results (p-value $\geq$ 0.05).

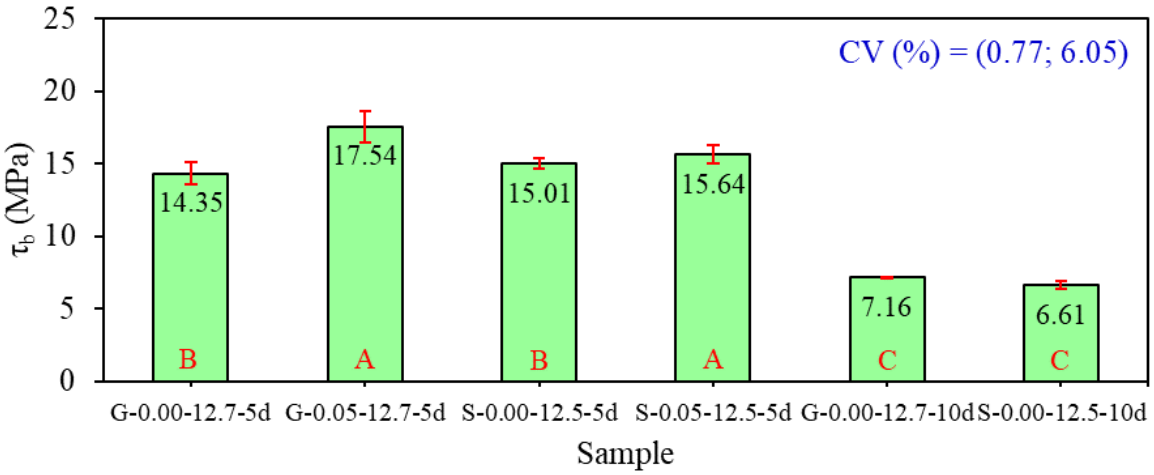

Figure 6: Pull-out test results

The results of Tukey's test showed that the maximum bond stress occurred in the concrete samples with an addition of 0.05% CNT, which may be linked to the higher compressive strength (Figure 5a) and lower porosity (Figure 5e) of these samples compared to plain concrete. Specifically, in the samples with CNTs, τ_b was 22% and 4% higher than in the reference samples with GFRP and steel bars, respectively, with statistically significant differences. Tukey's test also indicated that the bar type did not significantly influence τ_b, resulting in equivalent means in the samples with or without CNTs.

Regarding the anchoring length, very relevant differences were noted. Precisely, in the samples with 10d anchorage length, τ_b was 50% and 56% lower than in those with 5d anchorage length.

In terms of the failure mode, it was observed that all specimens experienced pullout failure, confirming that a C/d ratio greater than 5 is more prone to result in pullout failure. It is worth mentioning that the ribs of the GFRP bars were deformed (by shear) in the direction of the pullout force, which did not occur with the steel bars, as shown in Figure 6.

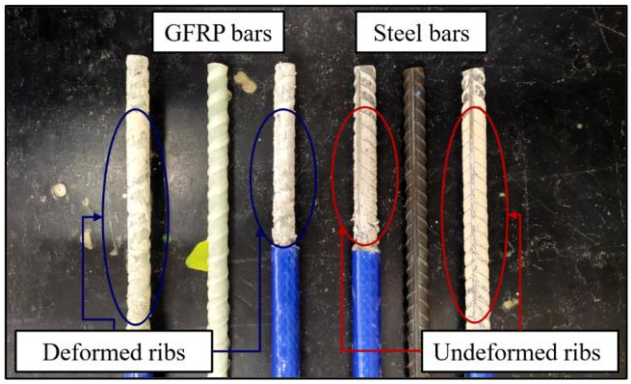

Figure 6: GFRP and steel bars pulled from the specimens

Considering aspects of strength, durability, weight, and corrosion resistance, this research brings satisfactory results about using GFRP bars over steel ones. It can also be said that considering the proposed cylindrical specimens, the anchorage length of 5d, recommended by the RILEM-RC-5 standard (RILEM, 1982) and commonly employed by the literature (Qasem et al., 2020; Song et al., 2020), is sufficient to ensure uniform distribution of stresses between the grout and the concrete.

CONCLUSIONS

This research evaluated the bond behavior of GFRP bars in CNT-concrete and its mechanical and durability properties. The following conclusions can be drawn:

i. The addition of 0.05% CNT resulted in an 12% increase in CS and a 26% increase in TS, while the addition of 0.10% CNT showed even more significant improvements with a 23% increase in CS and a 29% increase in TS.
ii. The CNT addition to the cement matrix did not significantly affect the values of Es and Ed.
iii. Incorporating 0.05% CNT into the concrete led to reductions of 18% and 16% in P and WA, respectively, compared to plain concrete. On the other hand, adding 0.10% CNT did not show further significant improvements.
iv. The bond strength (τ_b) in samples with CNTs was significantly higher than in reference samples. The bar type did not importantly influence τ_b in all samples. Notably, a longer anchorage length (10d) led to significantly lower τ_b than the 5d anchorage length.

These conclusions refer to the CNT dispersion method employed, which proved to be effective, and to the cylindrical samples used. Another point that deserves attention is that the millimeter difference between the diameters of the GFRP and steel bars should have been evaluated. Based on these findings, future research directions are conducting pull-out tests using different bar diameters, surface types, and cubic specimens. Additionally, investigating other durability properties like ultrasonic pulse velocity, electrical resistivity, and mass loss due to acid attack is also suggested.

REFERENCES

ABNT (1998). NBR NM 67: Concreto – Determinação da consistência pelo abatimento do tronco de cone. Rio de Janeiro: Associação Brasileira de Normas Técnicas.

ABNT (2018). NBR 5739: Concreto – Ensaio de compressão de corpos de prova cilíndricos. Rio de Janeiro: Associação Brasileira de Normas Técnicas.

ABNT. (1987). NBR 9776: Agregados – Determinação da massa específica de agregados miúdos por meio do frasco de Chapman. Rio de Janeiro: Associação Brasileira de Normas Técnicas.

ABNT. (2003). NBR NM 248: Agregados – Determinação da composição granulométrica. Rio de Janeiro: Associação Brasileira de Normas Técnicas.

ABNT. (2009). NBR 9778-2: Argamassa e concreto endurecidos – Determinação da absorção de água, índice de vazios e massa específica. Rio de Janeiro: Associação Brasileira de Normas Técnicas.

ABNT. (2011). NBR 7222: Concreto e argamassa – Determinação da resistência à tração por compressão diametral de corpos de prova cilíndricos. Rio de Janeiro: Associação Brasileira de Normas Técnicas.

ABNT. (2015a). NBR 8953: Concreto para fins estruturais: Classificação por grupo de resistência. Rio de Janeiro: Associação Brasileira de Normas Técnicas.

ABNT. (2021). NBR 8522-1: Concreto endurecido – Determinação dos módulos de elasticidade e de deformação. Rio de Janeiro: Associação Brasileira de Normas Técnicas.

Ahmed, H., Bogas, J. A., Guedes, M., & Pereira, M. F. C. (2019). Dispersion and reinforcement efficiency of carbon nanotubes in cementitious composites. *Magazine of Concrete Research*, *71*(8), 408-423.

Benmokrane, B., Mousa, S., Mohamed, K., & Sayed-Ahmed, M. (2021). Physical, mechanical, and durability characteristics of newly developed thermoplastic GFRP bars for reinforcing concrete structures. *Construction and Building Materials*, *276*, 122200.

Boudjehm, H., Bouteldja, F., Nafa, Z., & Bendjaiche, R. (2022). Hardened properties of pre-cracked concrete incorporating metakaolin and crushed blast furnace slag as an additional blend material. *Construction and Building Materials*, *352*, 129009.

Carvalho, E. P., Miranda, M. P., Fernandes, D. S., & Alves, G. V. (2018). Comparison of test methodologies to evaluate steel-concrete bond strength of thin reinforcing bar. *Construction and Building Materials*, *183*, 243-252.

Chuah, S., Li, W., Chen, S. J., Sanjayan, J. G., & Duan, W. H. (2018). Investigation on dispersion of graphene oxide in cement composite using different surfactant treatments. *Construction and Building Materials*, *161*, 519-527.

De Fazio, D., Boccarusso, L., Formisano, A., Viscusi, A., & Durante, M. (2023). A Review on the Recycling Technologies of Fibre-Reinforced Plastic (FRP) Materials Used in Industrial Fields. *Journal of Marine Science and Engineering*, *11*(4), 851.

Ferro, G., Tulliani, J. M., Lopez, A., & Jagdale, P. (2015). New cementitious composite building material with enhanced toughness. *Theoretical and applied fracture mechanics*, *76*, 67-74.

Gillani, S. S. U. H., Khitab, A., Ahmad, S., Khushnood, R. A., Ferro, G. A., Saleem Kazmi, S. M., Qureshi, L. A., & Restuccia, L. (2017). Improving the mechanical performance of cement composites by carbon nanotubes addition. *Procedia Structural Integrity*, *3*, 11-17.

Han, Y., Shao, S., Fang, B., Shi, T., Zhang, B., Wang, X., & Zhao, X. (2023). Chloride ion penetration resistance of matrix and interfacial transition zone of multi-walled carbon nanotube-reinforced concrete. *Journal of Building Engineering*, 106587.

Hassan, A., Elkady, H., & Shaaban, I. G. (2019). Effect of adding carbon nanotubes on corrosion rates and steel-concrete bond. *Scientific Reports*, *9*(1), 6285.

Jung, M., Lee, Y. S., Hong, S. G., & Moon, J. (2020). Carbon nanotubes (CNTs) in ultra-high performance concrete (UHPC): Dispersion, mechanical properties, and electromagnetic interference (EMI) shielding effectiveness (SE). *Cement and Concrete Research*, *131*, 106017.

Konsta-Gdoutos, M. S. M. S., Danoglidis, P. A., & Shah, S. P. S. P. (2019). ESSEHigh modulus concrete: Effects of low carbon nanotube and nanofiber additions. Theoretical and Applied Fracture Mechanics, 103, 102295.

Liew, K. M., Kai, M. F., & Zhang, L. W. (2016). Carbon nanotube reinforced cementitious composites: An overview. *Composites Part A: Applied Science and Manufacturing*, *91*, 301-323.

Liu, S., Bai, C., Zhang, J., Zhao, K., Li, Q., & Jin, G. (2023). Experimental study on bonding performance of GFRP bars-recycled aggregate concrete under sulfate attack environment. *Construction and Building Materials*, *379*, 131231.

Makar, J. M., & Chan, G. W. (2009). Growth of cement hydration products on single-walled carbon nanotubes. *Journal of the American Ceramic Society*, *92*(6), 1303-1310.

Martins, J. V., Aguilar, M. T. P., Garcia, D. C. S., & dos Santos, W. J. (2022). Management and characterization of concrete wastes from concrete batching plants in Belo Horizonte–Brazil. *Journal of Materials Research and Technology*, *20*, 1157-1171.

Mendes, J. C., Moro, T. K., Figueiredo, A. S., do Carmo Silva, K. D., Silva, G. C., Silva, G. J. B., & Peixoto, R. A. F. (2017). Mechanical, rheological and morphological analysis of cement-based composites with a new LAS-based air entraining agent. *Construction and Building Materials*, *145*, 648-661.

Qasem, A., Sallam, Y. S., Hossam Eldien, H., & Ahangarn, B. H. (2020). Bond-slip behavior between ultra-high-performance concrete and carbon fiber reinforced polymer bars using a pull-out test and numerical modelling. *Construction and Building Materials, 260*, 119857

Rabbani, A., Jamshidi, S., & Salehi, S. (2014). An automated simple algorithm for realistic pore network extraction from micro-tomography images. *Journal of Petroleum Science and Engineering*, *123*, 164-171.

Raza, A., & Rafique, U. (2021). Efficiency of GFRP bars and hoops in recycled aggregate concrete columns: Experimental and numerical study. *Composite Structures*, *255*, 112986.

Reis, E. D., de Azevedo, R. C., Christoforo, A. L., Poggiali, F. S. J., & Bezerra, A. C. S. (2023). Bonding of steel bars in concrete: A systematic review of the literature. *Structures*, *49*, 508-519.

Rocha, V. V., & Ludvig, P. (2018). Nanocomposites prepared by a dispersion of CNTs on cement particles. *Architecture, Civil Engineering, Environment*, *11*(2), 73-77.

Sinkhonde, D., Onchiri, R. O., Oyawa, W. O., & Mwero, J. N. (2022). Durability and water absorption behaviour of rubberised concrete incorporating burnt clay brick powder. *Cleaner Materials*, *4*, 100084.

Song, X. B., Cai, Q., Li, Y. Q., & Li, C. Z. (2020). Bond behavior between steel bars and carbon nanotube modified concrete. *Construction and Building Materials, 255*, 119339.

Stratus, 2021. Vergalhões em fibras de vidro – FRP rebars. Stratus: Ficha de Informação Técnica.

Van Tonder, P., & Mafokoane, T. T. (2014). Effects of multi-walled carbon nanotubes on strength and interfacial transition zone of concrete. *Construction Materials and Structures*, 718-727.

Vieira, L. D. B. P., de Figueiredo, A. D., Moriggi, T., & John, V. M. (2019). Waste generation from the production of ready-mixed concrete. *Waste management*, *94*, 146-152.

Wenner, F. (1916). *A method of measuring earth resistivity* (No. 258). US Government Printing Office.

Wu, L., Huang, G., & Liu, W. V. (2021). Methods to evaluate resistance of cement-based materials against microbially induced corrosion: A state-of-the-art review. *Cement and Concrete Composites*, *123*, 104208.

Wu, X., Chen, L., Li, H., & Xu, J. (2019). Experimental study of the mechanical properties of reinforced concrete compression members under the combined action of sustained load and corrosion. *Construction and Building Materials*, *202*, 11-22.

Xiong, Z., Wei, W., Liu, F., Cui, C., Li, L., Zou, R., & Zeng, Y. (2021). Bond behaviour of recycled aggregate concrete with basalt fibre-reinforced polymer bars. *Composite Structures*, *256*, 113078.

Xu, S., Liu, J., & Li, Q. (2015). Mechanical properties and microstructure of multi-walled carbon nanotube-reinforced cement paste. *Construction and Building Materials, 76*, 16–23.

Yu, A. P., Naqvi, M. W., Hu, L. B., & Zhao, Y. L. (2020). An experimental study of corrosion damage distribution of steel bars in reinforced concrete using acoustic emission technique. *Construction and Building Materials, 254*, 119256.

ACKNOWLEDGEMENT
The authors acknowledge the funding support from CEFET-MG and the material donation from Supermix and EMFAL.

CONFLICT OF INTEREST
The authors declare that they have no conflicts of interest associated with the work presented in this paper.

DATA AVAILABILITY
Data on which this paper is based is available from the authors upon reasonable request.